Progress In Electromagnetics Research C, Vol. 37, 1–13, 2013

AN L-PROBE FED STACKED RECTANGULAR MICROSTRIP ANTENNA COMBINED WITH A RING ANTENNA FOR TRIPLE BAND OPERATION IN ITS

Takafumi Fujimoto* **and Daisuke Tanaka**

Graduate School of Engineering, Nagasaki University, 1-14 Bunkyo, Nagasaki 852-8521, Japan

Abstract—A stacked rectangular microstrip antenna with a shorting plate combined with a rectangular ring microstrip antenna is proposed for triple band operation (GPS, VICS and ETC) in ITS. The two microstrip antennas are excited by an L-probe feed. In the ETC band, axial ratio deteriorates due to asymmetrical distributions of the electric current in the ring microstrip antenna. In this paper, an approach to improve the axial ratio for ETC is also proposed. The proposed antenna has the proper radiation patterns and impedance matching for the GPS, VICS and ETC.

1. INTRODUCTION

ITS (Intelligent Transport System) has received much attention as a system for traffic safety and environmental protection. ITS applications such as ETC (electric toll collection system), GPS (global positioning system), SDRAS (satellite digital audio radio service) and VICS (vehicle information and communications system) have been proposed and are widely used presently. In order to use all these applications, multi band antennas represent an effective solution as car antennas for the ITS. In the ITS, a circularly polarized wave is used in the ETC, SDRAS and GPS, while a linearly polarized wave in the VICS. Therefore, car antennas have to radiate both circularly polarized waves and linearly polarized waves. In [1, 2], dual band microstrip antennas (MSAs) with two feed ports for ITS have been proposed. However, in the design for antennas with the multi feed ports, the isolations between the feed ports have to be reduced, which makes the design of the antenna difficult.

Received 9 December 2012, Accepted 23 January 2013, Scheduled 24 January 2013

* Corresponding author: Takafumi Fujimoto (takafumi@nagasaki-u.ac.jp).

The authors have proposed a single feed stacked MSA with a shorting plate as a car antenna for VICS and ETC [3]. In the ETC band, the proposed antenna radiates a circularly polarized wave at high elevation angles where the toll gate antennas are installed. In the VICS band, the antenna can receive signals with uniform level within the communication area [3, 4]. In this paper, an antenna combining a stacked MSA proposed in [3] and a ring MSA is proposed as a car antenna for triple band operation in ITS. The stacked MSA in [3] is excited at the lower patch by a coaxial feed through the lower dielectric substrate. In this paper, an L-probe feed is used to excite two antennas, a stacked MSA and a ring MSA. A MSA fed by L-probe has been proposed by Guo et al. for wideband operation [5]. Moreover, Lau and Luk have proposed a dual-band circularly polarized MSA fed by four L-probes [6]. However, as mentioned above, the isolations between the feed ports have to be reduced in the design for antennas with multi feed ports. MSAs fed by a single L-probe which can radiate circularly polarized waves in multi band have not yet been reported, to the best of the authors' knowledge.

For the simulations in this paper, the simulation software package XFDTD ver. 7, which is based on the finite difference time domain method (FDTD), is used. In order to ascertain the accuracy of the simulated results, the simulated VSWR, axial ratio, radiation pattern and gain are compared with experimental data.

2. SPECIFICATIONS OF GPS, VICS AND ETC

In GPS, antennas have to receive signals from at least four satellites at any one time [7]. Therefore, it is desirable that the car antenna for GPS radiates at wide angles. The communication area for VICS extends 35 m in both directions from the beacon antenna installed at the shoulder of the road. In such a case, the radiation peak of the car antenna must be at low elevation angles along the road [3, 4]. Figure 1 shows an ETC system. The communication area for ETC extends 4 m in one direction from the toll gate antenna which is installed above the car antenna. Therefore, it is desirable that the car antenna for ETC radiates at $0^\circ \leqq \alpha \leqq 40^\circ$ in the yz plane only in the $+y$ direction and $0^\circ \leqq \beta \leqq 10^\circ$ in the xz plane. The center frequency and the bandwidth of GPS are 1.575 GHz and 2 MHz. Those of VICS in Japan are 2.4997 GHz and 85 kHz. Those of ETC in Japan are 5.8 GHz and 75 MHz. In order to keep high communication quality for a mobile communication system such as ITS, it is desirable for the bandwidth to be as wide as possible. In this paper, therefore, bandwidths of 10 MHz, 40 MHz and 100 MHz are aimed for in the GPS, the VICS

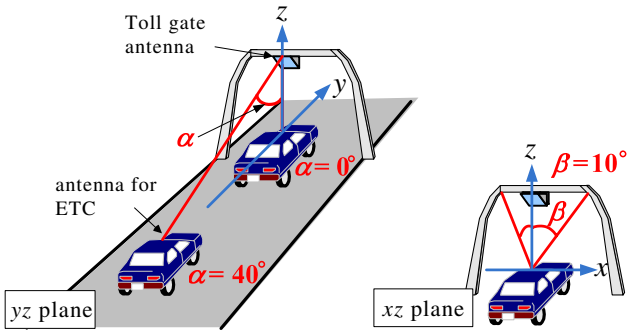

Figure 1. ETC system (Electric toll collection system).

and the ETC bands, respectively. Linear polarization is used for VICS while circular polarization is used for GPS and ETC.

3. ANTENNA DESIGN

Figure 2 shows a proposed triple band MSA. The antenna consists of a stacked rectangular patch MSA and a rectangular ring MSA. The two antennas are excited by an L-probe feed. The microstrip line of the L-probe feed lies around the diagonal of the rectangular patches and the rectangular ring. Although the upper and lower rectangular patches are the same size, the slits are installed on the lower patch to reduce the size of the stacked MSA and to achieve the circularly polarized wave in the ETC band. Similarly, the T-shaped slits are installed at each edge of the rectangular ring to reduce the size of the ring MSA and to achieve the circularly polarized wave in the GPS band. The upper patch is shorted to the lower patch at the apex by a conducting plate to obtain the resonance in the VICS band [3, 4]. In order to control the radiation pattern and the axial ratio in the ETC band, moreover, two rectangular elements are installed at a plane where the microstrip line lies. In this paper, the elements are referred to as Rc-elements (radiation's control elements).

The geometrical parameters optimized for GPS, VICS and ETC is shown in Table 1. The relative dielectric constants of each layer are $\varepsilon_{r1} = 1.0$, $\varepsilon_{r2} = 2.15$ and $\varepsilon_{r3} = 2.6$. In single layered MSAs, as the thickness of the dielectric substrate increases, the bandwidth increases [8]. Therefore, the height of the ring MSA is determined to satisfy the specification of the bandwidth of GPS. In the VICS and ETC bands, the bandwidths increase as the height of the upper patch of the stacked MSA increases [3]. Therefore, the height of the upper patch is determined to satisfy the specifications of the bandwidths of

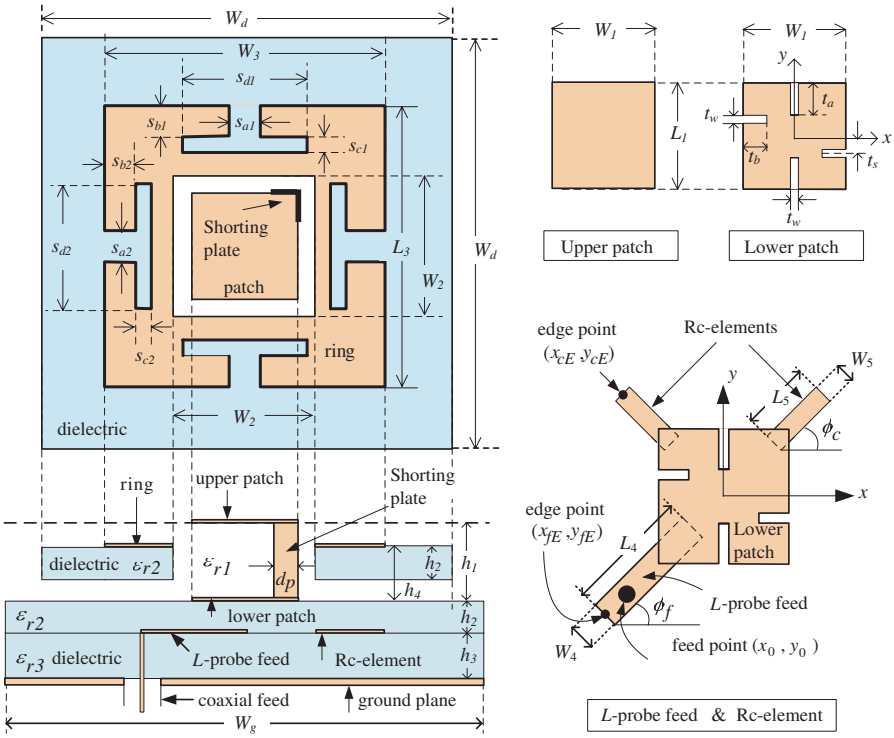

Figure 2. Geometry of a proposed antenna.

Table 1. Optimized geometrical parameters (units of ϕ_f and ϕ_c are degree and the others are mm).

W_1	L_1	W_2	W_3	L_3	W_4	L_4	W_5	L_5
13.6	15.1	19.0	40.4	42.4	4.24	28.04	4.24	10.9
h_1	h_2	h_3	h_4	t_a	t_b	t_w	t_s	W_d
4.0	0.8	1.6	1.6	2.55	3.6	0.4	5.2	50
s_{a1}	s_{a2}	s_{b1}	s_{b2}	s_{c1}	s_{c2}	s_{d1}	s_{d2}	W_g
4.0	6.73	2.81	2.81	5.75	4.93	19.4	19.0	100
d_p	x_{fE}	y_{fE}	x_0	y_0	x_{cE}	y_{cE}	ϕ_f	ϕ_c
1.5	−18	−18	−17	−17	−13.5	14.5	40.7	43

both VICS and ETC. The impedance matching in the three frequency bands are tuned by adjusting the positions of the feed point (x_0, y_0) and the edge point (x_{fE}, y_{fE}), the width W_4, the length L_4 and the angle ϕ_f of the microstrip line. In simulations and measurements in Sections 4 and 5, the optimized geometrical parameters are used.

4. OPERATIONAL PRINCIPLES IN TRIPLE BAND

Figure 3 shows the simulated VSWRs of the proposed MSAs with and without Rc-elements, and a stacked MSA without either Rc-elements or a ring MSA.

The stacked MSA without the ring MSA has two resonant modes in the VICS and the ETC bands [3]. However, the stacked MSAs combined with a ring MSA, regardless of inclusion of the Rc-elements, have a new resonant mode in the GPS band. Therefore, it is seen that the ring MSA operates as a radiation element in the GPS band. Figure 4(a) shows time averaged electric current distribution at the frequency giving the minimum axial ratio in the GPS band. It is confirmed that the electric current flows strongly on the ring MSA and the electric currents exist around only the edges of the lower patch and the shorting plate in the stacked MSA with a shorting plate. The dimension of the T-shaped slits along the x-axis is different from that along the y-axis. Moreover, a microstrip line of the L-probe feed lies around the diagonal of the rectangular ring. Therefore, the ring MSA with the T-shaped slits radiates a circularly polarized wave with the

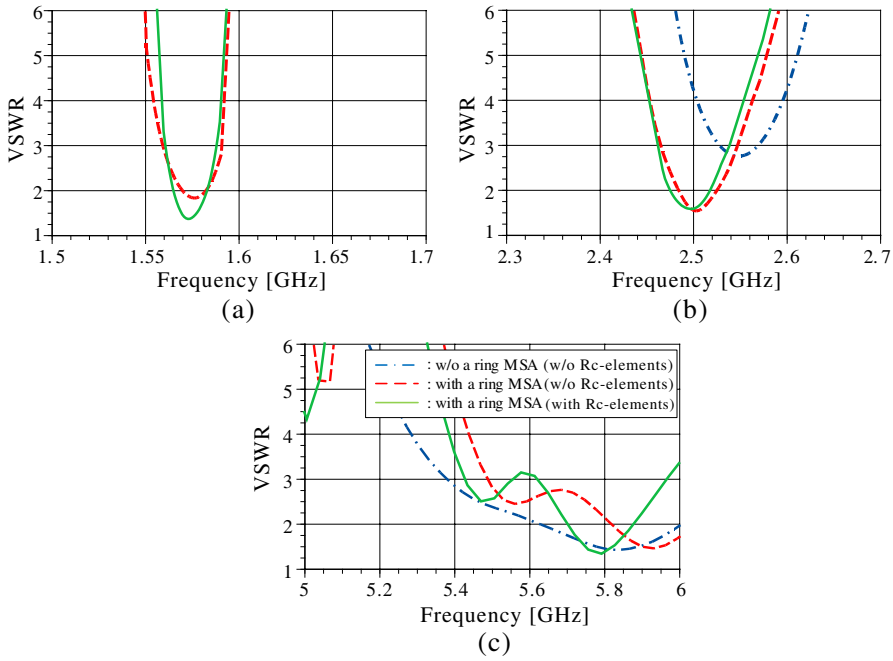

Figure 3. Simulated VSWRs of stacked MSAs with and without ring MSA. (a) GPS band. (b) VICS band. (c) ETC band.

appropriate size of each geometric parameter of the T-shaped slits and with the appropriate ratio (L_3/W_3) of the length to the width of the rectangular ring. The ring MSA operates as a single feed MSA with perturbation segments for circular polarization.

In the VICS band, the difference of the VSWR between the stacked MSAs with and without the ring MSA is very small. This states that the stacked MSA operates as a radiation element in the same principle as the antenna proposed in [3]. Figure 4(b) shows time averaged electric current distribution at the frequency giving the minimum VSWR in the VICS band. In the stacked MSA with a shoring plate, the intensities of the electric current around the shorting plate are maximum and those on the opposite apexes to the shorting plate are approximately zero on the upper and lower patches. The antenna resonates when the sum of the lengths of the diagonal of the upper and lower patches and the shorting plate becomes a half wavelength.

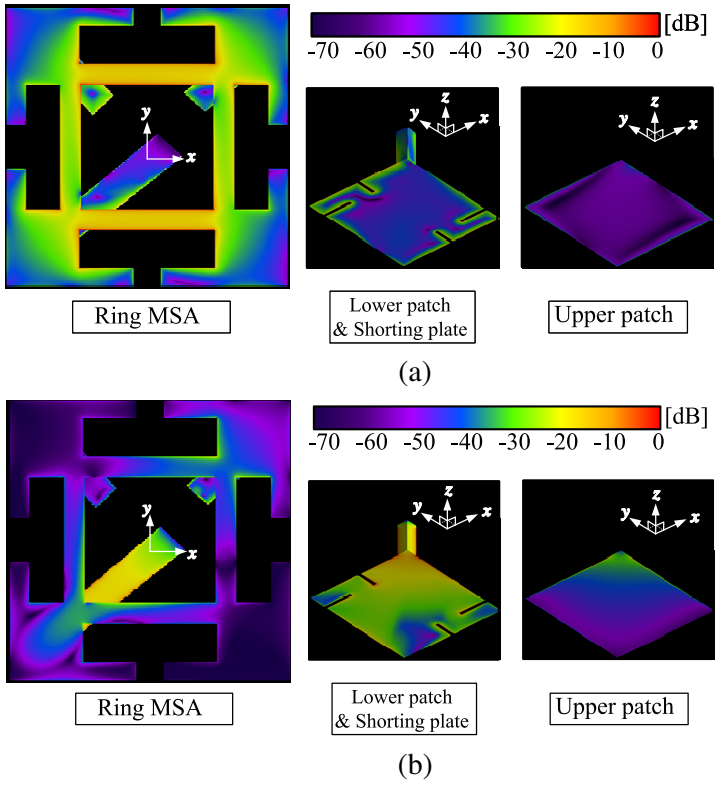

Figure 4. Time averaged electric current distributions in GPS and VICS bands. (a) GPS band (1.574 GHz). (b) VICS band (2.498 GHz).

Although the intensities of the electric current on the ring MSA are very small compared with those on the shoring plate, the electric currents flow on the ring MSA in the vicinity of the shorting plate and above the microstrip line of the L-probe feed.

It is confirmed from Figure 3 that the ring MSA influences the VSWR not only in the GPS band but also in the ETC band. Figure 5(a) shows time averaged electric current distribution of the antenna without the Rc-elements at frequency giving the minimum axial ratio in the ETC band. Without the Rc-elements, the electric current flows strongly on the ring MSA above the L-probe feed. The electric current distribution on the ring MSA significantly affects the axial ratio in the ETC band. In order to improve the symmetry of the electric current distribution on the ring MSA in the ETC band, two Rc-elements are installed on the upper left and the upper right on

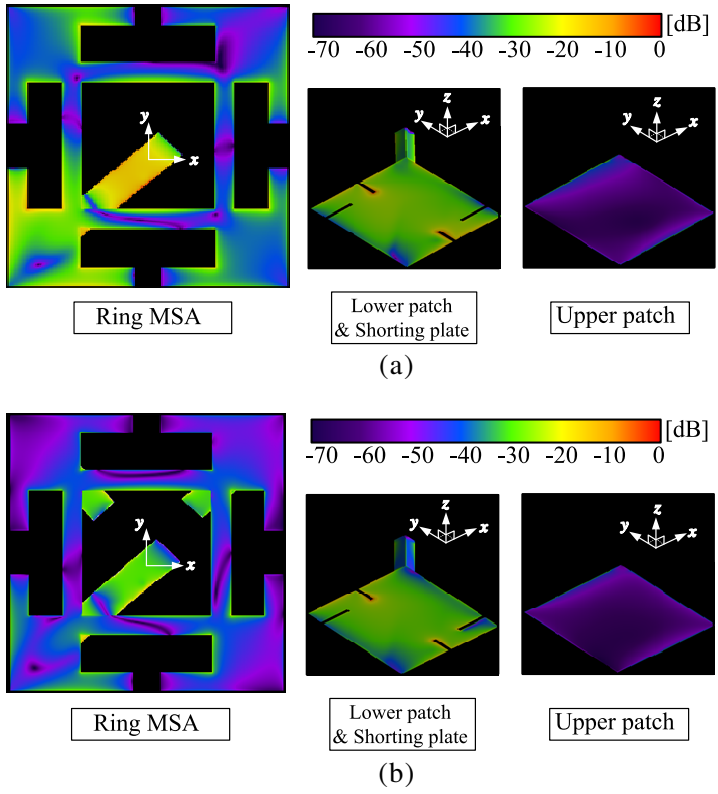

Figure 5. Time averaged electric current distributions in ETC band. (a) Without Rc-elements (5.81 GHz). (b) With Rc-elements (5.79 GHz).

the plane where the microstrip line lies. The two Rc-elements are the same size and are arranged symmetrically with respect to the y-axis. Figure 5(b) shows the electric current distribution of the antenna with the Rc-elements. The electric current on the ring MSA above the L-probe feed becomes very small and concentrates on the lower patch and

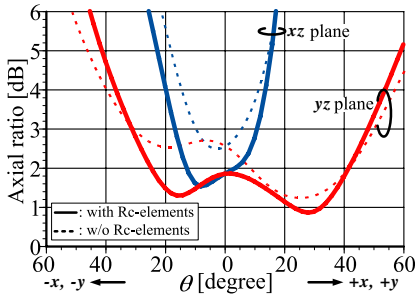

Figure 6. Simulated axial ratios for change of elevation angle θ (w/o Rc-elements: 5.81 GHz, with Rc-elements: 5.79 GHz).

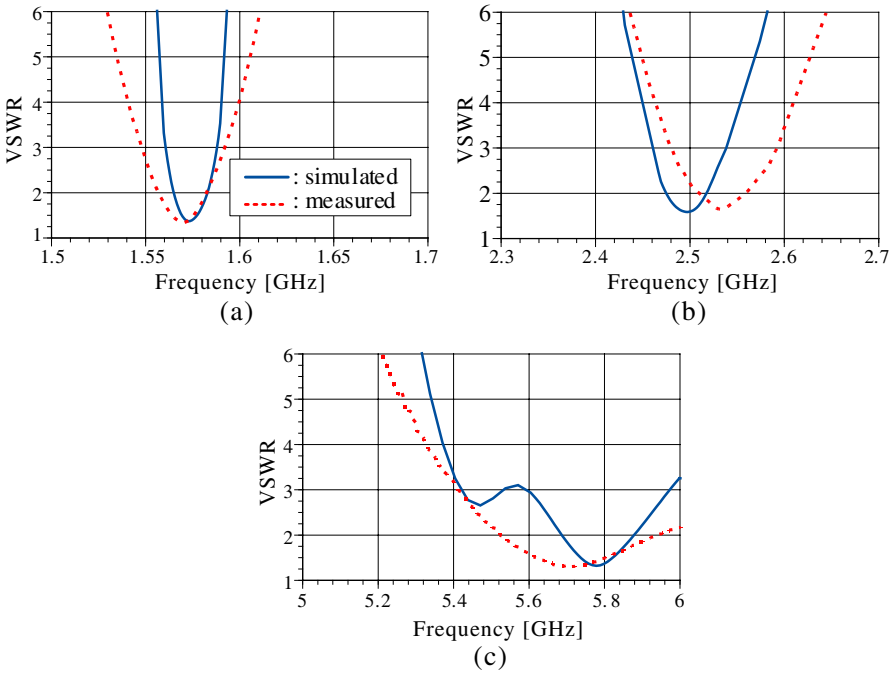

Figure 7. Simulated and measured VSWRs. (a) GPS band. (b) VICS band. (c) ETC band.

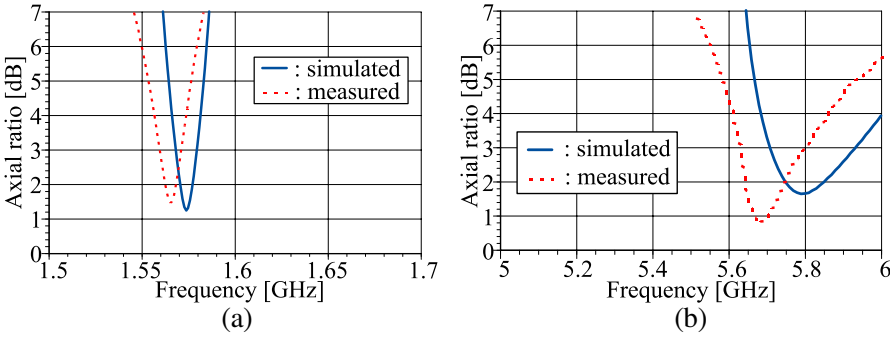

Figure 8. Simulated and measured axial ratios. (a) GPS band. (b) ETC band.

the Rc-elements. Figure 6 shows the simulated axial ratio against the change of elevation angle θ at the frequency giving the minimum axial ratio. By installing the Rc-elements, the axial ratio for the elevation angle is improved.

In [9], a circularly polarized MSA with a slit at the center of each edge of the rectangular patch has been proposed. In the antenna fed by the L-probe, however, the slits overlap the microstrip line of the L-probe feed. Therefore, it is difficult to tune the impedance matching in the VICS and ETC bands simultaneously. In this paper, the slits along the x-axis are deviated by t_s from the center of the edge of the rectangular patch.

5. ANTENNA CHARACTERISTICS

Figures 7 and 8 show the measured and simulated VSWRs and the axial ratios, respectively. The antenna was made of copper-clad Glass-fiber-PTFE. The measured bandwidths (VSWR $\leqq$ 2 with axial ratio $\leqq$ 3 dB) in the GPS and ETC bands are 11.5 MHz and 165 MHz, respectively. The measured bandwidth (VSWR $\leqq$ 2) in the VICS band is 43 MHz. The fabricated antenna satisfies the specification of the bandwidths in the triple band. The relative errors of the center frequency between the simulated and measured results in the GPS, VICS and ETC bands are 0.57%, 1.40% and 1.83 %, respectively. The measured center frequencies agree well with the simulated ones.

Figures 9(a)–(c) show the measured and simulated radiation patterns normalized by the maximum value of the electric fields in the xz and yz planes. As shown in Figures 7 and 8, since the measured VSWR and axial ratio against frequency don't agree completely with

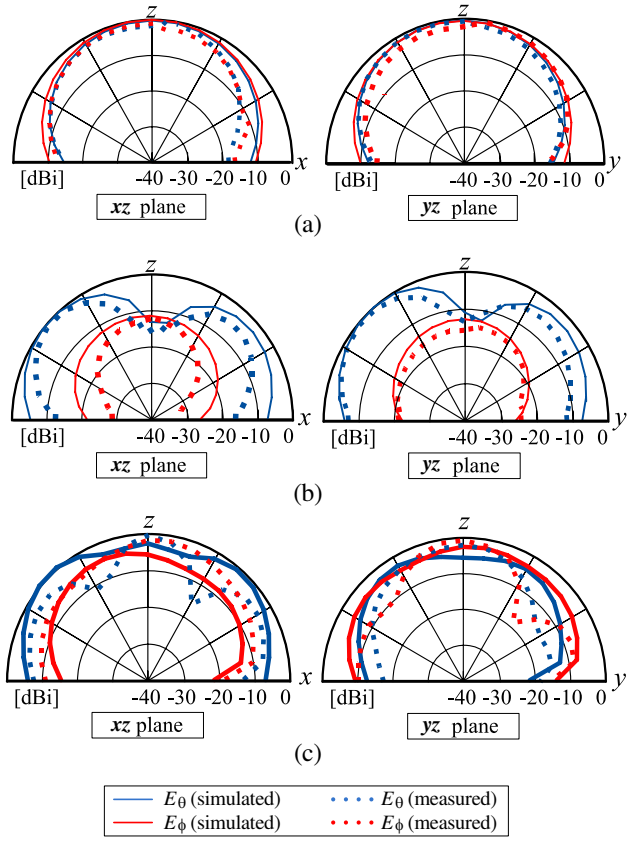

Figure 9. Simulated and measured radiation patterns. (a) In GPS band (simulated: 1.574 GHz, measured: 1.565 GHz). (b) In VICS band (simulated: 2.498 GHz, measured: 2.532 GHz). (c) In ETC band (simulated: 5.79 GHz, measured: 5.68 GHz).

the simulated results. Therefore, in the GPS and ETC bands, the simulated radiation patterns are compared with the measured ones at the frequency giving the minimum axial ratio. In the VICS band, the simulated radiation pattern is compared with the measured one at the frequency giving the minimum VSWR. In the GPS band, the simulated angles of axial ratio $\leqq 3$ dB are approximately $0^\circ \leqq \theta \leqq 85^\circ$ in the both xz and yz planes. In the VICS band, the radiation peak is at a low elevation angle, which is very similar to the radiation pattern of the antenna proposed in [3]. These radiation patterns match the required ones for GPS and VICS. In the ETC band, a null exists around $\theta = 30^\circ$ in the measured results.

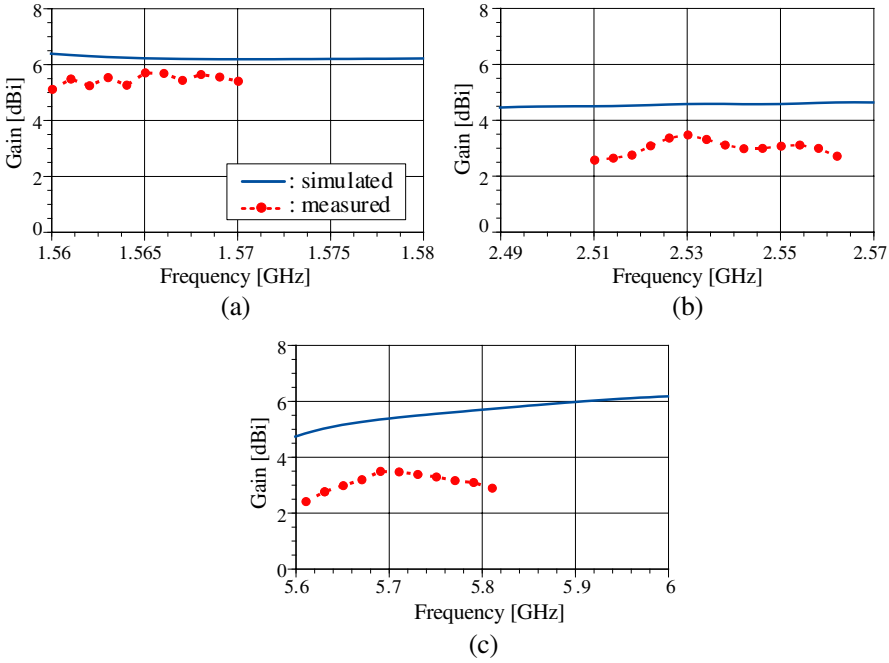

Figure 10. Simulated and measured gains. (a) GPS band. (b) VICS band. (c) ETC band.

Figures 10(a) and (c) show the simulated and measured gains at $\theta = 0°$ in the GPS and ETC bands. The measured results are shown in the frequency range where the axial ratio is 3.0 dB or less. Figure 10(b) shows the simulated and measured gains at the elevation angle $\theta = 45°$ where both the simulated and the measured gains are maximum at the frequency giving the minimum VSWR. The measured results are shown in the frequency range where the VSWR is 2 or less. In the GPS band, the measured gains agree with the simulated results in the whole frequencies with the axial ratio $\leqq 3$ dB. In the VICS band, the simulated maximum gain (4.41 dBi) agrees with the simulated one (3.45 dBi). However, the measured results vary between 2.50 dBi and 3.45 dBi in the frequency range. In the ETC band, the errors between the simulated and the measured gains are big compared to those in the GPS band. Since the electric currents exist on the ring MSA in the VICS and ETC bands as mentioned in the previous section, the ring MSA contributes to radiation in the VICS and ETC bands. Therefore, aberration of the position of these two antennas during fabrication affects the radiation pattern and gains in the VICS and ETC bands.

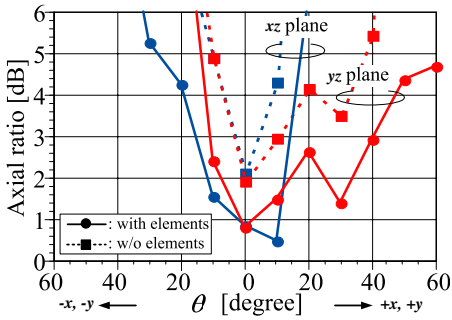

Figure 11. Measured axial ratios for change of elevation angle θ (w/o Rc-elements: 5.97 GHz, with Rc-elements: 5.68 GHz).

The radiation angle of circularly polarized waves is very important for ETC. However, as shown in Figure 9(c), there are differences between the simulated and measured radiation patterns. Therefore, the axial ratio for changes of the angles is investigated. Figure 11 shows the measured axial ratio for changes of elevation angles θ in the xz and yz planes. The measured values of the antenna without the Rc-elements are shown for comparison. The angles with the axial ratio $\leqq 3$ dB are approximately $\theta = 40°$ in the yz plane ($y > 0$) and $\theta = 10°$ in the xz plane. Although differences between the simulated results (Figure 6) and the measured results are observed, the antenna with the Rc-elements satisfies the specifications for the angle distributions of the axial ratio mentioned in the Section 2.

6. CONCLUSION

An L-probe fed stacked MSA combined with a ring MSA has been proposed for triple band (GPS, VICS and ETC) operation in ITS.

The operational principles of the antenna were discussed. Moreover, the antenna characteristics (VSWR, axial ratio, radiation pattern and gain) were simulated and compared with measured results. In the simulation, the proposed antenna satisfies the specifications of the impedance matching and axial ratio and has suitable radiation patterns. Although differences between the simulated and measured radiation patterns in the ETC band were observed, the measured angle distributions of the axial ratio satisfy the ETC specification. There were differences between the measured and simulated center frequencies in the triple band, too. However, the relative errors between the simulated and measured center frequencies were small in

the triple band. Although the geometry of the proposed antenna is complicated, the measured results of the center frequencies present the correct operation of the prototype antenna.

REFERENCES

1. Rafi, G. Z., M. Mohajer, A. Malarky, P. Mousavi, and S. Safavi-Naeini, "Low-profile integrated microstrip antenna for GPS-DSRC application," *IEEE Antennas Wireless Propag. Lett.*, Vol. 8, 44–48, 2009.
2. Wei, K., Z. Zhang, and Z. Feng, "Design of a coplanar integrated microstrip antenna for GPS-DSRC application," *IEEE Antennas Wireless Propag. Lett.*, Vol. 8, 458–461, 2011.
3. Fujimoto, T. and K. Tanaka, "Stacked rectangular microstrip antennas with a shorting plate for dual band (VICS/ETC) operation in ITS," *IEICE Trans. Commun.*, Vol. E90-B, No. 11, 3307–3310, 2007.
4. Fujimoto, T., S. Noguchi, T. Tanaka, and M. Taguchi, "Stacked square microstrip antenna with a shorting post for road vehicle communication," *RF and Microwave Computer-aided Engineering*, Vol. 14, No. 3, 244–252, 2004.
5. Guo, Y. X., C. L. Mak, K. M. Luk, and K. F. Lee, "Analysis and design of L-probe proximity fed-patch antennas," *IEEE Trans. Antennas and Propag.*, Vol. 49, No. 2, 145–149, Feb. 2001.
6. Lau, K. L. and K. M. Luk, "A wide-band circularly polarized L-probe coupled patch antenna for dual-band operation," *IEEE Trans. Antennas and Propag.*, Vol. 53, No. 8, 2636–2644, Aug. 2005.
7. Chen, X., C. G. Parini, B. Collins, Y. Yao, and M. U. Rehmanm, *Antennas for Global Navigation Satellite Systems*, John Wiley & Sons, Chichester, 2012.
8. Waterhouse, R. B., *Microstrip Patch Antennas: A Designer's Guide*, Kluwer Academic Publishers, Boston, 2003.
9. Wong, K. L. and J. Y. Wu, "Single-feed small circularly polarized square microstrip antenna," *Electron. Lett.*, Vol. 33, No. 22, 1833–1834, Oct. 1997.